Chemosphere 194 (2018) 340–351

Contents lists available at ScienceDirect

Chemosphere

journal homepage: www.elsevier.com/locate/chemosphere

Differential sensitivity of light-harnessing photosynthetic events in wheat and sunflower to exogenously applied ionic and nanoparticulate silver

P. Pardha-Saradhi [a], [*], Nisha Shabnam [b], P. Sharmila [c], Ashok K. Ganguli [c], [d], Hyunook Kim [b], [**]

[a] *Department of Environmental Studies, University of Delhi, Delhi, 110007, India*
[b] *Department of Environmental Engineering, University of Seoul, Seoul, 02504, South Korea*
[c] *Department of Chemistry, Indian Institute of Technology, New Delhi, 110016, India*
[d] *Institute of Nanoscience and Technology, Habitat Centre, Phase-X, Sector-64, Mohali, 160062, Punjab, India*

HIGHLIGHTS

- Ag-NPs, unlike Ag$^+$, do not perturb light harnessing photosynthetic machinery.
- Ag-NPs, unlike Ag$^+$, do not perturb polyphasic Chl a fluorescence transients.
- Photosynthetic events in wheat than in sunflower are more sensitive to Ag$^+$.
- Uptake of ionic Ag by plants is significantly higher than nanoparticulate Ag.
- Ag$^+$ is translocated to leaves in wheat, but detained by the stem in sunflower.

ARTICLE INFO

Article history:
Received 9 September 2017
Received in revised form
19 November 2017
Accepted 22 November 2017
Available online 22 November 2017

Handling Editor: Shane Snyder

Keywords:
Ag$^+$
AgNPs
Photosystem II
Chl a fluorescence kinetics
Triticum aestivum
Helianthus annuus

ABSTRACT

Potential impacts of inevitable leaks of silver nanoparticles (AgNPs) into environment on human beings need attention. Owing to the vitality of photosynthesis in maintaining life and ecosystem functioning, impacts of exogenously applied nanoparticulate and Ag$^+$ on photosystem (PS)II function, which governs overall photosynthesis, in wheat and sunflower were evaluated. PSII efficiency and related Chl *a* fluorescence kinetics of these two plants remained unaffected by AgNPs. However, Ag$^+$ caused a significant decline in the PSII activity and related fluorescence steps in wheat, but not in sunflower. Electron flow between Q_A and PQ pool was found most sensitive to Ag$^+$. Number of active reaction centers, electron transport, trapping of absorbed light for photochemistry, and performance index declined, while dissipation of absorbed light energy as heat significantly increased in wheat exposed to Ag$^+$. Total antioxidant activity in sunflower was least affected by both Ag and AgNPs. In contrast, in the case of wheat, the antioxidant activity was declined by Ag$^+$ but not by AgNPs. Further, the amount of silver absorbed by plants exposed to Ag$^+$ was higher than that absorbed by plants exposed to AgNPs. While wheat retained majority of Ag in its roots, sunflower showed major Ag accumulation in stem. Photosynthetic events in sunflower, unlike wheat, were least affected as no detectable Ag levels was recorded in their leaves. Our findings revealed that AgNPs seemed non/less-toxic to light harnessing photosynthetic machinery of wheat, compared to Ag$^+$. Photosynthetic events in sunflower were not affected by Ag$^+$, either, as its translocation to leaves was restricted.

Abbreviations: ABS, absorbed energy flux; Chl, chlorophyll; CSo, cross section or leaf area; DIo, energy flux dissipated as heat; EDX, energy dispersive X-ray; ETo, electron transport; Fv, variable fluorescence; Fm, maximal fluorescence; OJIP, polyphasic fast Chl *a* fluorescence transients, where O and P refer to minimal and maximal fluorescence, and J and I are inflections between O and P; PQ, plastoquinone; PS II, photosystem II; Q_A, Quinone; RC, reaction center; TRo, trapping of absorbed light energy; ϕPo, quantum yield of primary photochemistry (Fv/Fm); ψEo, Quantum yield of electron transport; SAED, selected area electron diffraction; TEM, transmission electron microscope.

[*] Corresponding author.

[**] Corresponding author.

E-mail addresses: ppsaradhi@gmail.com (P. Pardha-Saradhi), h_kim@uos.ac.kr (H. Kim).

https://doi.org/10.1016/j.chemosphere.2017.11.122
0045-6535/

1. Introduction

Silver nanoparticles (AgNPs) are the most widely used engineered NPs. Owing to their exceptional physicochemical and antimicrobial properties, AgNPs find immense applications in engineering, medicine, agriculture and environment (Rai et al., 2009; Fabrega et al., 2011; Yamal et al., 2013; Shabnam et al., 2016). This has led to a rapid and tremendous increase in demand-based production and usage of AgNPs. Indeed, AgNPs have become an integral part of consumer products such as cosmetics, textiles, hospitals, food packaging industries, water purification, paints, etc. that are commonly used in our daily life (Rai et al., 2009; Pardha-Saradhi et al., 2014; Arruda et al., 2015). Release of NPs into the environment from various consumer products has been reported earlier (Benn and Westerhoff, 2008; Kaegi et al., 2010; Gondikas et al., 2014; Kunniger et al., 2014). Based on previous records, Ellis et al. (2018) recently reported that (i) the annual production of nano-products increased from 10 tons in 2011 to 300 tons in 2015; and (ii) estimated levels of AgNPs in sediments, sludge, treated soils and surface water are 30.1 mg kg^{-1}, 2.3 mg kg^{-1}, 2.3 mg kg^{-1} and 2.2 mg L^{-1}, respectively. The inevitable release of AgNPs into our surroundings and apprehensions of its likely negative impact(s) on living beings including humans have drawn attention of scientists, policy makers and regulatory bodies (e.g., World Health Organization, Environmental Protection Agencies, European Commission etc.) (Duvall and Wyatt, 2011). The established findings revealing negative impacts of AgNPs on mammalian cells including human ones further add to the concern on potential leaks of AgNPs into environment; accordingly, impact of metal-NPs on living systems has been being investigated by researchers across the globe for over a decade. AgNPs cause toxicity to mammalian skin, liver, lung, brain, vascular system and reproductive organs (Nel et al., 2006; Ahamed et al., 2010). These AgNPs can induce genes associated with cyclic progression of cells to get damaged, resulting in complete cell apoptosis (Ahamed et al., 2010).

Significant work has been carried out on impacts of AgNPs on both freshwater and marine biota which include daphnids, fish, etc. (Navarro et al., 2008; Chae et al., 2009; Zhao and Wang, 2011; Lapresta-Fernandez et al., 2012; Oukarroum et al., 2012, 2013). Similarly, enormous work has been carried out to evaluate the impact of AgNPs on a variety of microorganisms: in particular, a negative impact on the integrity of plasma membrane (Bao et al., 2015). Although there are numerous studies on impact of AgNPs on plants, most of these are fragmentary or limited to few growth parameters (such as seed germination, length and fresh/dry weight of root/shoot), inadequate anatomical studies, F_v/F_m, Chl content, transpiration and some components of an antioxidant system (Stampoulis et al., 2009; Gubbins et al., 2011; Jiang et al., 2012; Sharma et al., 2012; Yin et al., 2012, 2012; Qian et al., 2013; Yasur and Rani, 2013; Nair and Chung, 2014). Some of these studies showed positive/non-inhibitory effects of AgNPs on growth of a few plant species (Yin et al., 2011; Sharma et al., 2012; Vannini et al., 2014; Yasur and Rani, 2013; Zuverza-Mena et al., 2016). In contrast, there are also reports on negative impacts of AgNPs on plants (Lin and Xing, 2007; Kumari et al., 2009; Stampoulis et al., 2009; Yin et al., 2011; Qian et al., 2013; Thuesombat et al., 2014; Zuverza-Mena et al., 2016). The AgNPs induced negative impact is believed to be mediated through the release of Ag ions (Vannini et al., 2014; Arruda et al., 2015). Ag^+-induced negative impact may be related to its potential to replace Cu from Cu-containing/dependent biomolecules/receptors such as the ethylene (an important and only gaseous key plant growth regulator) receptor (McDaniel and Binder, 2012; Shabnam et al., 2017).

Recently, it was reported that ionic silver (i.e., Ag^+) is more toxic to light harnessing photosynthetic machinery of *Spirodela polyrhiza*, an aquatic plant, than AgNPs (Shabnam et al., 2017). Photosynthesis is the key metabolic event that governs plant growth (or development) and overall productivity (Shabnam and Pardha-Saradhi, 2016; Shabnam et al., 2017). It is well established that the CO_2 fixation and productivity of a plant rely largely on the light harvesting photosynthetic machinery, in particular PS II (Shabnam et al., 2017; Shabnam and Pardha-Saradhi, 2016). Hence, in the present study, the impact of exogenously applied AgNPs and Ag^+ on light harnessing photosynthetic events in two distinct crop plants, namely, wheat (an important cereal crop) and sunflower (an important oil yielding crop) was evaluated. In this communication, we report for the first time that (i) nanoparticle species of Ag do not have any negative impact on the light harnessing photosynthetic machinery and antioxidant potential; and (ii) wheat responds differentially to Ag^+ compared to sunflower based on a significant variation in translocation of Ag ions into their leaves.

2. Materials and methods

Seeds of *Triticum aestivum* L. (cv. 1544) (wheat, Poaceae) were obtained from the Indian Agricultural Research Institute (Delhi, India). Seeds of *Helianthus annuus* L. (DRSF-108) (sunflower, Asteraceae) were obtained from the Directorate of Oil Seeds Research, Hyderabad (Telangana, India).

2.1. Synthesis and harvest of silver nanoparticles

Silver nanoparticles were prepared by autoclaving 0.5 mM $AgNO_3$ supplemented with 0.1% yeast extract at 121 °C under a pressure of 1.06 kg cm^{-2} for 20 min (Yamal et al., 2013). Subsequent to cooling the solution; AgNPs were harvested through centrifugation at 28000 × *g*. The pellet obtained was then washed with deionized. The later was achieved through steps involving resuspension of the pellet in deionized water and centrifugation at least three times. Subsequently, the resultant washed AgNP pellet was dried in a desiccator at room temperature and homogenized to obtain a fine uniform powder. A 1000 ppm (i.e., 1000 mg L^{-1}) stock solution was prepared by sonicating the suspension of fine powder of AgNPs in deionized distilled water through 30 min sonication at 33 khZ in a Metrex ultra-sonic bath sonicator (Metrex Scientific Instruments Pvt., Delhi, India). Investigation with TEM coupled with EDX and SAED revealed that majority of AgNPs were in the size range of 20–30 nm (Fig. 1).

2.2. Exposure of crop plants to Ag^+ and AgNPs

Various concentrations of AgNPs were prepared using 1000 ppm AgNPs stock solution. Grains/seeds of wheat and sunflower were washed with cetrimide, treated with 0.1% $HgCl_2$ for 5 min, washed thoroughly with sterilized double-distilled water, and then were placed in autoclaved glass bottles containing glass beads in double-distilled water, in a laminar hood. These bottles were then incubated under continuous light (with an intensity of 120 μmol photons m^{-2} s^{-1}) at 25 ± 2 °C. 10 days old uniform plants of wheat and sunflower were selected and their root system was washed carefully with sterile distilled water. The selected seedlings were exposed independently to different levels (0, 10, 25, 50 and 100 ppm) of AgNPs and Ag^+ ($AgNO_3$ was used for preparing different levels of Ag^+) by immersing their root system in respective test solutions in Borosil glass test tubes (125 × 12 mm). Then, the plants were incubated under continuous light (with an intensity of 120 μmol photons m^{-2} s^{-1}) at 25 ± 2 °C for 24 h. No agglomeration of AgNPs was noted during these experiments.

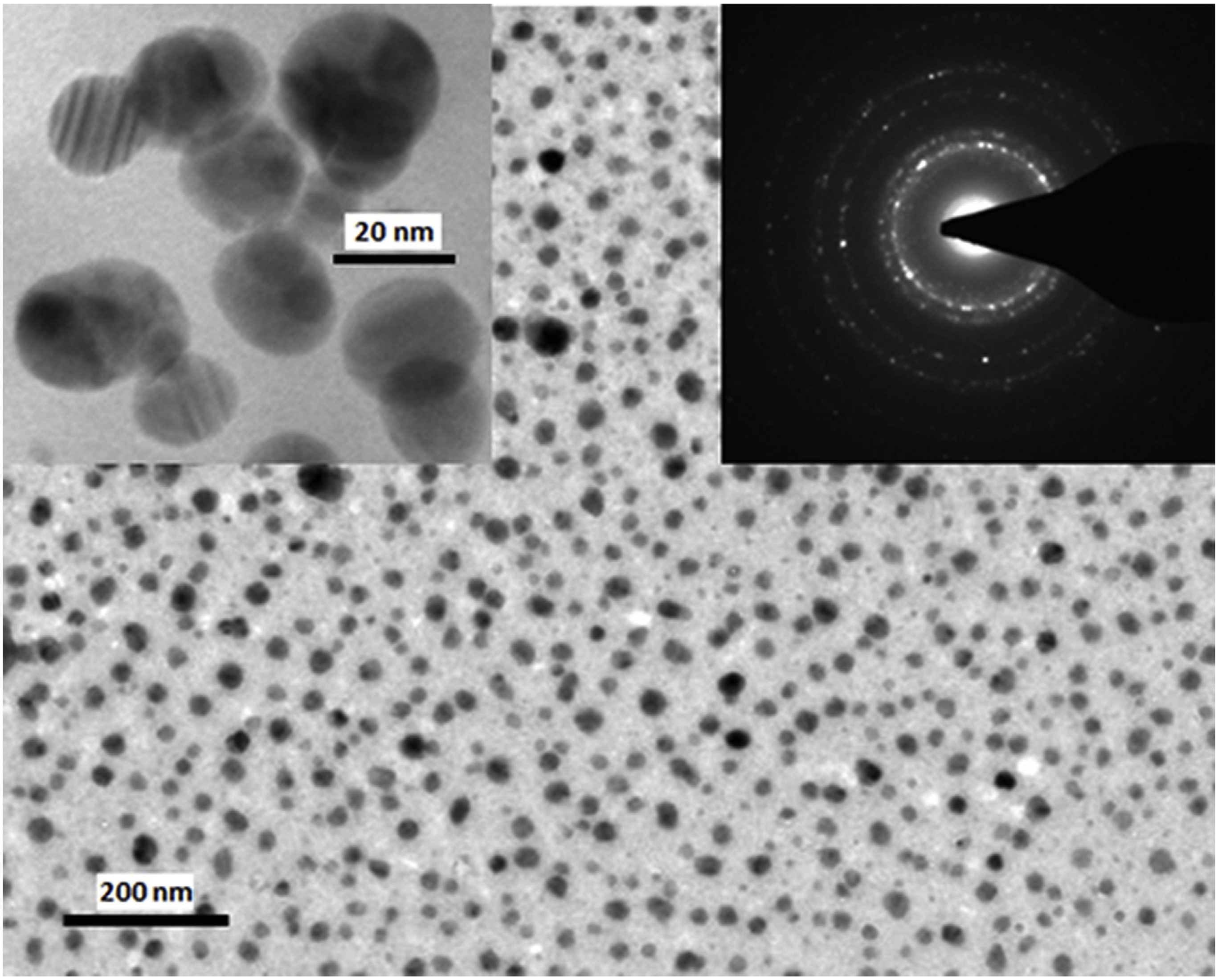

Fig. 1. Transmission electron micrographs of AgNPs. Insets on left and right represent magnified view and selected area electron diffraction pattern of AgNPs, respectively.

2.3. Impact of AgNPs and Ag^+ on light harnessing photochemical reactions

The impact of exogenously applied AgNPs and Ag^+ on light harnessing photochemical reactions in leaves of wheat and sunflower was evaluated using a plant efficiency analyzer (Handy PEA; Hansatech, Norfolk, UK). Wheat and sunflower plantlets exposed to varying levels of Ag^+ and AgNPs for 24 h were dark-adapted for 40 min and used for recording PS II efficiency and fluorescence kinetics as described in Shabnam et al. (2015). Biolyzer Software HP 3, which was developed by Strasser and Strasser (1995) (Bioenergetics Laboratory, Geneva, Switzerland) was used for plotting Chl *a* fluorescence transients. This software relies on the well-known JIP test for plotting Chl *a* fluorescence transients and translates original Chl *a* fluorescence measurements into various biophysical and phenomenological expressions. It can be used as a powerful tool for evaluating overall behavior of various components of the photosynthetic machinery involved in photochemical reactions (Strasser et al., 2004; Kalaji et al., 2011; Chen et al., 2016).

The biophysical and phenomenological expressions considered in the present study include (i) dissipation at the level of antenna Chl (DI_o/RC) [which is equal to (ABS/RC)-(TR_o/RC)]; (ii) electron transport per reaction center (ET_o/RC); (iii) the maximum quantum yield of primary photochemistry ($TR_o/ABS = F_v/F_m$); (iv) the quantum yield of electron transport ($\Psi_o = ET/TR_o$); (v) absorption per excited cross section (CS) (ABS/CS_o); (vi) the fraction of active PSII reaction centers per excited CS (RC/CS_o); (vii) trapping per excited CS (TR_o/CS_o); (viii) electron transport per excited CS (ET_o/CS_o); and (ix) dissipation per excited CS (DI_o/CS_o). A more detailed explanation can be found in Zhang et al. (2015) and Strasser et al. (2004). All experiments were carried out eight times with two replicates.

Data are presented as mean ± standard error. The analysis of variance was performed with data from the experiments using RStudio (Version 1.0.44, RStudio Inc., Boston, MA, USA).

2.4. Quantification of antioxidant capacity

1,1-diphenyl-2-picrylhydrazyl (DPPH) radical scavenging assay following the modified protocol of Brand-Williams et al. (1995) was used for quantification of antioxidant capacity. To determine the impact of exogenously applied Ag^+ and AgNPs on total antioxidant activity in wheat and sunflower plantlets, the ethanol extract of the leaves of plantlets was mixed in equal proportion with 0.1 mM

DPPH dissolved in ethanol and incubated under ambient conditions in dark for 30 min. For a control, 0.1 mM DPPH dissolved in ethanol was mixed in an equal proportion with ethanol. Subsequently, light absorbance of the samples was read at 517 nm. DPPH scavenging activities of ethanol extracts of various plant samples were expressed in terms of nmoles of DPPH radical scavenged.

2.5. *Determination of silver content in plants*

Oven dried plant samples were acid-digested in HNO_3 at 100 ^{O}C for 20 min in a BUCHI Digest Automate K-438 (New Castle, DL, USA). The digested samples were then diluted with deionized water and filtered. A blank was prepared using deionized water and digested as stated above. Silver content was measured using an inductively coupled plasma (ICP) emission spectrometer (Schimazdu ICPE-9000, Kyoto, Japan). For quality control, readings of the blank as well as a standard were taken after measurement of every 10 samples.

All experiments were carried out eight times, each with three replicates. Data are presented as mean ± standard error. The analysis of variance was performed with the data from the experiments using RStudio (Version 1.0.44, RStudio Inc., Boston, MA, USA).

3. Results and discussion

3.1. *Impact of Ag^+ and AgNPs on light harnessing photosynthetic events*

Plant growth and development are largely linked to photosynthetic capacity (Shabnam et al., 2017). Therefore, we evaluated the impact of exogenously applied Ag^+ and AgNPs on key light harnessing photosynthetic events by measuring F_v/F_m. Previously, Navarro et al. (2008) observed AgNPs induced decline in PS II efficiency (measured in terms of F_v/F_m) in freshwater alga, *Chlamydomonas reinhardtii*.

Fig. 2 depicts PS II efficiency of wheat and sunflower exposed to Ag^+ and AgNPs. In corroboration with our earlier report (Shabnam et al., 2017), the plants exposed to AgNPs did not show any significant alteration in their PS II efficiency. Surprisingly, Ag^+ did not have any negative impact on PS II efficiency in sunflower, but induced rather a significant decline of the PS II efficiency in wheat at concentrations of >50 ppm (Fig. 2). Zhang et al. (2015) believed that F_v/F_m cannot be taken as a perfect indicator of primary photochemistry, i.e., PS II efficiency. Although Jiang et al. (2012) and Qian et al. (2013) evaluated the impact of AgNPs on F_v/F_m and Chl content, no in-depth analysis was carried out to evaluate the true impact of ionic and nanoparticulate silver on photochemical reactions in crop plants.

It is well established that Chl *a* fluorescence kinetics can be used as a good tool to determine PS II efficiency and overall photosynthesis of genotypes of same and different plant species exposed to different abiotic stresses (Vani et al., 2001; Zhang et al., 2015; Chen et al., 2016; Shabnam et al., 2017). Therefore, we evaluated the impact of exogenously applied Ag^+ and AgNPs on the Chl *a* fluorescence kinetics. The Chl *a* fluorescence transient of oxygenic organisms, on a logarithm time scale, shows a polyphasic nature with distinct OJIP steps (Shabnam et al., 2015, 2017). It is well established that O-J rise represents reduction of Q_A to Q_A^-, that J-I rise signifies reduction of PQ pool, and that I-P rise denotes reduction of acceptor

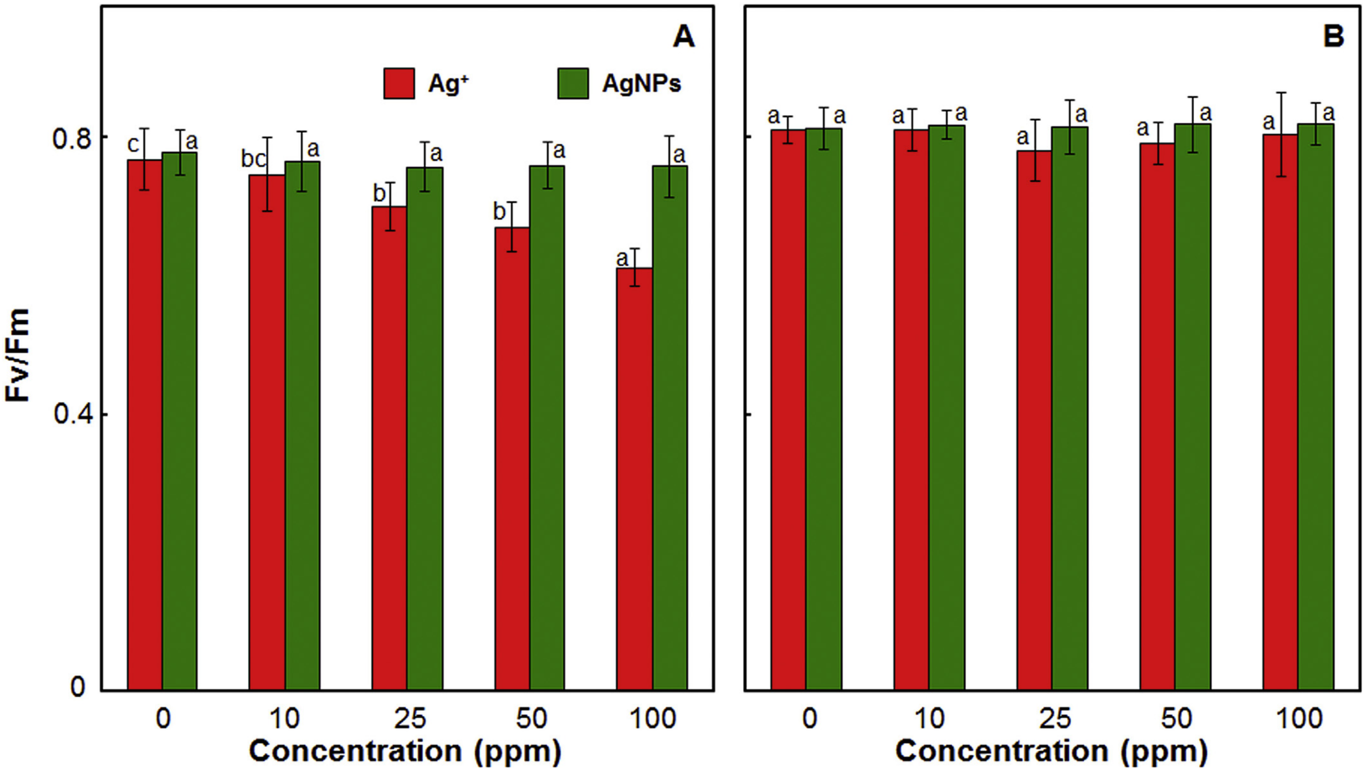

Fig. 2. Impact of exogenously applied ionic (Ag^+) (red bars) and nanoparticle (AgNPs) (green bars) species of silver on quantum yield of PS II activity (i.e., F_v/F_m) in leaves of wheat (*Triticum aestivum*) (A) and sunflower (*Helianthus annuus*) (B). Measurements were made after 24 h exposure of crop plants to varying levels of $AgNO_3$ and AgNPs. Values represent mean of data collected from eight independent experiments and vertical lines on bars represent standard error. Different small letters over the bars reflect that the values recorded for plants exposed to different concentrations (ppm) of Ag^+ or AgNPs differ significantly at $P < 0.05$ level (Duncan's multiple range test). (For interpretation of the references to colour in this figure legend, the reader is referred to the web version of this article.)

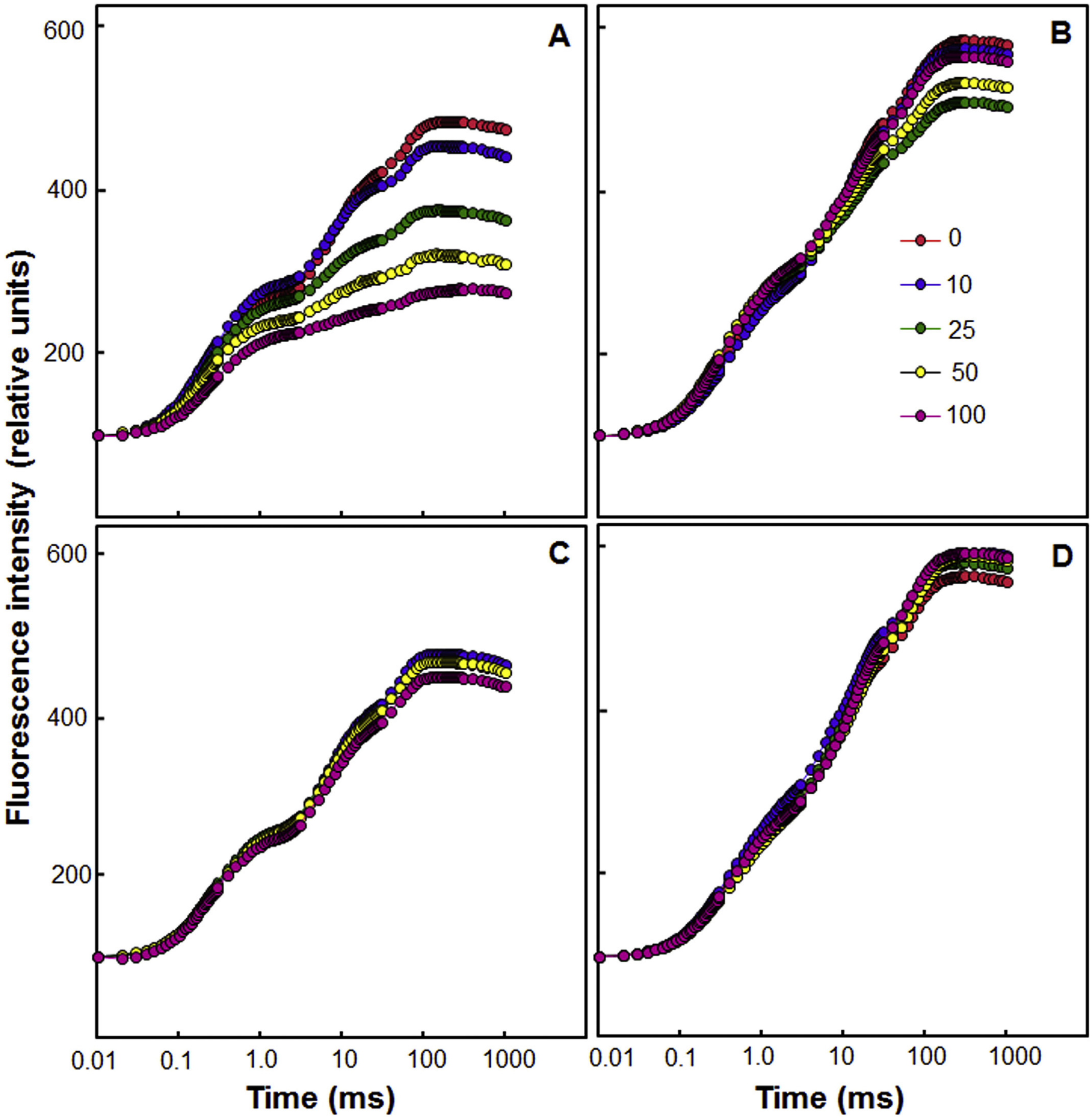

Fig. 3. Impact of exogenously applied ionic (Ag^+) (A, C) and nanoparticle (AgNPs) (B, D) species of silver on Chl *a* fluorescence transients (OJIP transients) of leaves of wheat (*Triticum aestivum*) (A, B), and sunflower (*Helianthus annuus*) (B, C). Measurements were made after 24 h exposure of crop plants to varying levels of $AgNO_3$ and AgNPs. Values represent mean of data collected from eight independent experiments.

side of PS I (Shabnam et al., 2015, 2017). Fig. 3 depicts the impacts of exogenously applied Ag^+ and AgNPs on Chl *a* fluorescence transients of wheat and sunflower leaves. As expected, both wheat and sunflower showed typical polyphasic Chl *a* fluorescence transients with distinct OJIP steps. As is evident from Fig. 3, Ag^+ brought about a significant decline in amplitude of Chl *a* fluorescence transients in wheat while it did not in sunflower. In contrast, exogenously applied AgNPs did not cause any negative impact on Chl *a* fluorescence transients in either of the plants compared to respective controls, even at the highest concentration tested, i.e., 100 ppm (Fig. 3). It is also clear from Fig. 4 that AgNPs did not cause any negative impact on O-J, J-I, and I-P steps, compared to respective controls. In contrast, all the three phases of Chl *a* fluorescence transients of wheat leaves showed a significant decline when the leaves were exposed to Ag^+. Interestingly, the decline in fluorescence amplitude by Ag^+ at the J-I step was more obvious compared to those at O-J and I-P steps (Fig. 4). These findings suggested that the transport of electrons between Q_A^- to PQ pool would be more prone to Ag^+ compared to other steps.

3.2. *Impact of exogenously applied Ag^+ and AgNPs on biophysical parameters related to harnessing light energy for photosynthesis*

Through the fluorescence kinetics, one can better understand the degree of sensitivity or tolerance of the key steps/components that govern the PS II function, which is the key regulator of overall photosynthesis (Strasser et al., 2004; Shabnam et al., 2017). In the present study, we have taken advantage of this software to precisely evaluate the impact of exogenously applied Ag^+ and AgNPs on a few vital biophysical steps associated with harnessing of light energy by PS II. The impact of exogenously applied Ag^+ and AgNPs on these biophysical steps associated with harnessing light energy for electron transport in wheat and sunflower are summarized in Tables 1 and 2 and Figs. 5 and 6. The expressions that are used in the present investigations are (i) phenomenological fluxes/activities (per CS); (ii) specific fluxes/activities (per RC); (iii) quantum efficiencies (also called as quantum yield and flux ratios). These fluxes and yields take into account the energy flow right from the absorption of light/photons for electron transport to acceptor sites of PSI and to $NADP^+$ (Strasser and Strasser, 1995). ABS in Tables 1 and 2 refers to the amount of light absorbed by the antenna pigments which excite a Chl molecule. A part of the absorbed light energy is trapped by TR for reduction of Q_A to Q_A^- and the rest of it is dissipated as DI (Strasser and Strasser, 1995). Electron transport deals with reoxidation of Q_A^-via ET over a CS of active and inactive RCs (Strasser and Strasser, 1995).

In general, (i) phenomenological fluxes, namely absorption per excited CS (ABS/CS_o), the fraction of active PS II reaction centers per excited CS (RC/CS_o), trapping per excited CS (TR_o/CS_o), as well as ET per excited CS (ET_o/CS_o); (ii) specific fluxes namely ET per RC (ET_o/RC), trapping per reaction center (TR/RC_o) as well as (iii) quantum efficiencies, namely quantum yield of ET ($\Psi_o = ET/TR_o$) and the maximum quantum yield of the primary photochemistry (φP_o or $F_V/F_m = TR_o/ABS$) were affected severely by Ag^+ in wheat in a concentration-dependent manner. All the ANOVA test results show that there was a significant difference between the control and Ag^+ treatments for each photosynthetic parameter (Table 1); all the p values were <0.01. In contrast, sunflower exposed to Ag^+ did not show any significant alteration in these biophysical parameters.

Interestingly, both wheat and sunflower exposed to AgNPs did

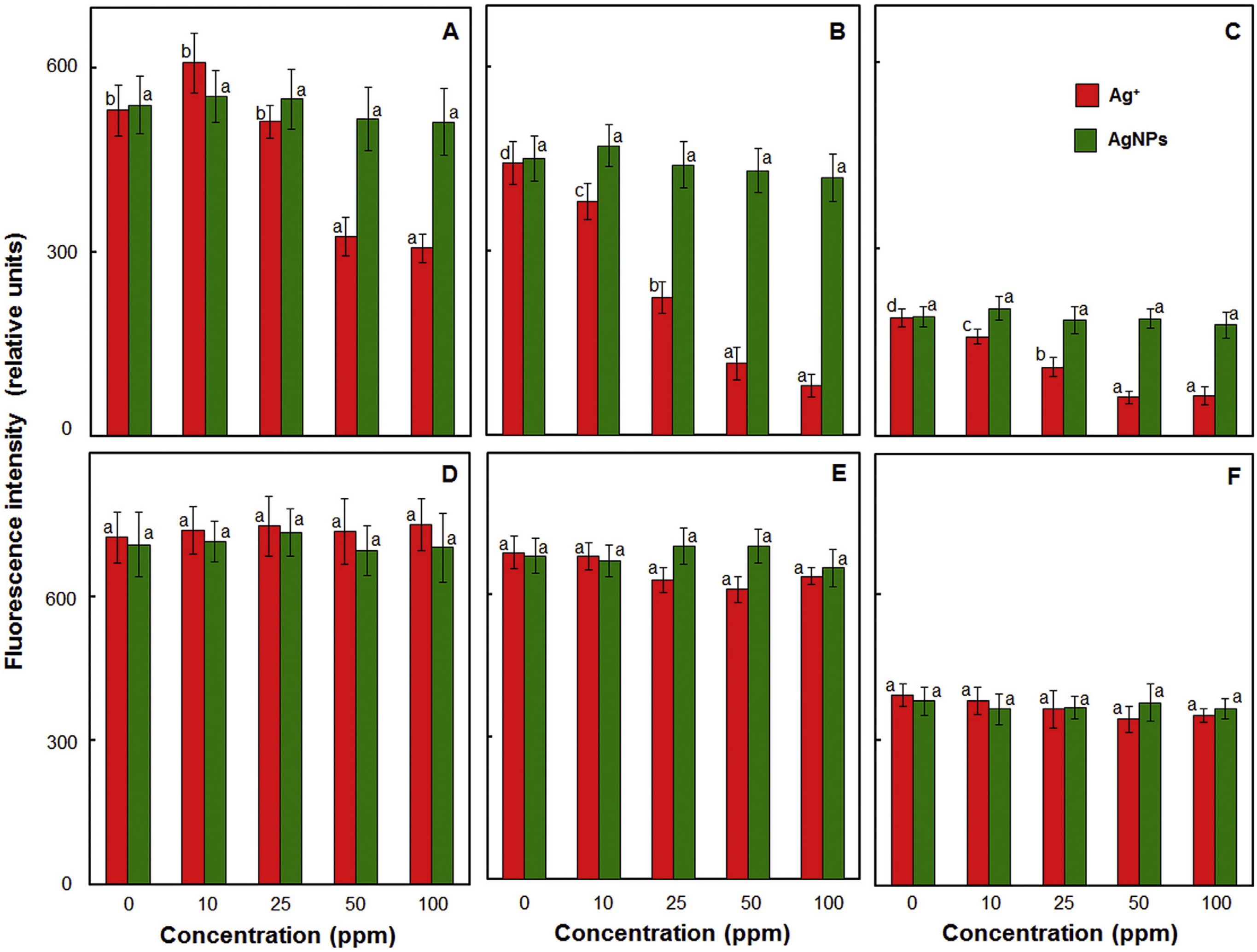

Fig. 4. Impact of exogenously applied ionic (Ag^+) (red bars) and nanoparticle (AgNPs) (green bars) species of silver on O-J (A,D), J-I (B,E) and I-P (C,F) stages of Chl *a* fluorescence transient curves of wheat (*Triticum aestivum*) (A–C) and sunflower (*Helianthus annuus*) (D–F). Measurements were made after 24 h exposure of crop plants to varying levels of $AgNO_3$ and AgNPs. Values represent mean of data collected from eight independent experiments and vertical lines on bars represent standard error. Different small letters over the bars reflect that the values recorded for plants exposed to different concentrations (ppm) of Ag^+ or AgNPs differ significantly at $P < 0.05$ level (Duncan's multiple range test). (For interpretation of the references to colour in this figure legend, the reader is referred to the web version of this article.)

Table 1

Impact of ionic and nanoparticulate species of silver on few key photosynthetic parameters in leaves of wheat plants. The data is derived from original Chl *a* fluorescence measurements through JIP test. The data is an average of at least eight independent recordings. Figures in parenthesis represent percent values with respect to controls.

Parameter	Control	Ionic silver (Ag^+), ppm				p[a]	Nanoparticulate species (Ag-NPs), ppm				p[a]
		10	25	50	100		10	25	50	100	
ETo/RC	1.258 (100)	1.178 (93.64)	1.049 (83.38)	1.002 (79.65)	0.729 (57.94)	7×10^{-12}	1.240 (98.56)	1.236 (98.25)	1.240 (98.56)	1.267 (100)	7.1×10^{-1}
DIo/RC	0.665 (100)	0.800 (120.30)	1.014 (152.48)	1.325 (199.24)	1.411 (212.18)	3×10^{-11}	0.647 (97.29)	0.692 (104.06)	0.669 (100.60)	0.698 (104.96)	1.1×10^{-1}
RC/CSo	122.332 (100)	124.136 (101.47)	108.288 (88.51)	83.496 (68.24)	82.591 (67.51)	2×10^{-8}	137.6479 (112.51)	132.413 (108.24)	123.668 (101.08)	122.988 (100.53)	1.9×10^{-1}
ABS/CSo	351.000 (100)	392.000 (111.68)	366.000 (104.27)	336.000 (104.27)	300.000 (85.47)	1×10^{-6}	379.000 (107.97)	378.000 (107.69)	361.000 (102.84)	355.000 (101.13)	2.3×10^{-1}
TRo/CSo	269.638 (100)	292.588 (108.51)	256.2000 (95.01)	225.321 (83.56)	183.420 (69.026)	7×10^{-12}	289.935 (107.52)	286.297 (106.18)	274.179 (101.68)	269.090 (99.79)	2.3×10^{-1}
ETo/CSo	153.936 (100)	146.294 (95.03)	108.603 (70.55)	87.627 (56.92)	60.235 (39.12)	7×10^{-14}	170.800 (110.95)	163.762 (106.38)	160.888 (104.51)	155.830 (101.23)	0.22×10^{-1}
DIo/CSo	81.361 (100)	99.411 (122.18)	109.800 (134.95)	110.678 (136.03)	116.580 (143.28)	7×10^{-5}	81.065 (99.63)	81.702 (100.41)	83.820 (103.02)	82.910 (101.9)	5.8×10^{-1}
Ψo = ET/TRo	0.5709 (100)	0.5000 (87.58)	0.4239 (74.25)	0.3889 (68.12)	0.3284 (57.52)	1×10^{-9}	0.5891 (103.18)	0.5720 (100.19)	0.5868 (102.78)	0.5791 (101.43)	9.9×10^{-1}
ϕ_{Po} = TRo/ABS	0.7682 (100)	0.7464 (97.16)	0.7000 (91.12)	0.6706 (87.29)	0.6114 (79.58)	2×10^{-8}	0.7650 (99.58)	0.7574 (98.59)	0.7595 (98.86)	0.7580 (98.67)	6.6×10^{-1}
PIABS	15.365 (100)	9.323 (60.67)	5.097 (33.17)	3.219 (20.95)	2.118 (13.78)	5×10^{-8}	16.954 (110.34)	15.614 (101.62)	16.108 (104.83)	14.931 (97.17)	3.1×10^{-2}

[a] p values calculated from the ANOVA test.

Table 2

Impact of ionic and nanoparticulate species of silver on few key photosynthetic parameters in leaves of sunflower plants. The data is derived from original Chl *a* fluorescence measurements through JIP test. The data is an average of at least eight independent recordings. Figures in parenthesis represent percent values with respect to controls.

Ameter	Control	Ionic silver (Ag^+), ppm				p[a]	Nanoparticulate species (Ag-NPs), ppm				p[a]
		10	25	50	100		10	25	50	100	
cETo/RC	1.072 (100)	0.967 (94.49)	0.984 (91.79)	1.000 (93.28)	0.987 (92.07)	4×10^{-1}	1.083 (90.20)	1.081 (93.37)	1.074 (94.40)	1.021 (95.24)	3.3×10^{-1}
DIo/RC	0.397 (100)	0.377 (94.96)	0.416 (104.8)	0.484 (121.91)	0.517 (130.23)	4×10^{-10}	0.343 (86.39)	0.348 (87.65)	0.335 (84.38)	0.341 (85.89)	1.1×10^{-1}
RC/CSo	198.73 (100)	204.80 (103.05)	199.66 (100.46)	186.67 (93.92)	179.84 (90.49)	2×10^{-1}	212.76 (103.05)	209.55 (107.44)	215.15 (108.26)	189.54 (95.37)	1.7×10^{-1}
ABS/CSo	418 (100)	424 (101.43)	426 (101.91)	463 (110.76)	399 (95.45)	4×10^{-1}	388 (92.82)	396 (94.73)	400 (95.69)	359 (85.88)	6.2×10^{-5}
TRo/CSo	339.00 (100)	343.65 (101.37)	333.05 (98.24)	366.23 (108.03)	321.08 (94.71)	3×10^{-1}	317.73 (93.72)	323.06 (95.29)	327.80 (96.69)	294.31 (86.81)	1.8×10^{-3}
ETo/CSo	213.16 (100)	215.57 (101.13)	184.36 (86.48)	193.57 (90.08)	177.01 (83.04)	6×10^{-5}	217.86 (102.20)	209.79 (98.41)	198.17 (92.96)	199.85 (93.75)	2.3×10^{-2}
DIo/CSo	79.02 (100)	80.35 (101.73)	92.95 (117.63)	96.77 (122.45)	97.92 (123.92)	1×10^{-3}	70.27 (88.92)	72.94 (92.30)	72.20 (91.36)	64.69 (81.86)	1.2×10^{-2}
Ψo = ET/TRo	0.628 (100)	0.627 (99.84)	0.574 (91.40)	0.545 (86.78)	0.531 (84.55)	7×10^{-6}	0.628 (100)	0.649 (103.34)	0.664 (105.73)	0.657 (104.61)	8.8×10^{-2}
ϕ_{Po} = TRo/ABS	0.811 (100)	0.810 (99.87)	0.781 (96.30)	0.791 (97.53)	0.804 (99.13)	7×10^{-1}	0.818 (100.86)	0.815 (100.49)	0.819 (100.98)	0.819 (100.98)	5.2×10^{-1}
PIABS	34.57 (100)	36.13 (104.45)	27.16 (78.57)	19.60 (56.70)	25.99 (75.19)	2×10^{-3}	39.55 (114.42)	43.42 (125.60)	48.39 (139.99)	46.14 (133.49)	2.2×10^{-4}

[a] p values calculated from the ANOVA test.

not show any alteration in these biophysical parameters (see Figs. 5 and 6 and Tables 1 and 2). These observations are in coherence with that with Chl *a* fluorescence transients (Fig. 3). The level/degree of assimilatory power generated and CO_2 fixation are inversely proportional to the amount of absorbed light dissipated as heat. Hence, the stress-induced decline in photosynthetic efficiency is associated with an increase in DI_o (Kalaji et al., 2011; Shabnam et al., 2017). Contrary to the significant suppression in biophysical steps associated with the use of trapped light energy for generating assimilatory power, Ag^+ treatment caused a significant enhancement in dissipation of absorbed light energy as heat (both DI_o/RC and DI_o/CS_o) in wheat but not in sunflower (Tables 1 and 2). Again, both sunflower and wheat exposed to AgNPs showed insignificant variation in both DI_o/RC and DI_o/CS_o, compared to respective controls (Tables 1 and 2).

Another important parameter derived from Chl *a* fluorescence through the JIP test is the performance index (PI_{ABS}) which is considered to be a marker of plant vitality (Kalaji et al., 2011; Strasser and Strasser, 1995); usually, the PI_{ABS} values decline under stress (Kalaji et al., 2011). While Ag^+ caused a significant decline in PI_{ABS} of wheat, no significant impact was observed in sunflower. However, neither of these crop plants showed any significant alteration in PI_{ABS} when they were exposed to AgNPs. These results clearly revealed that Ag^+ would significantly curtail the potential of wheat in using absorbed light energy for photochemical reactions, compared to AgNPs. This clearly shows that Ag^+ is more toxic to light harvesting photosynthetic events than AgNPs.

3.3. Impact of exogenously applied Ag^+ and AgNPs on antioxidant capacity

Recently, it was reported that leaves of *Potamogeton nodosus*

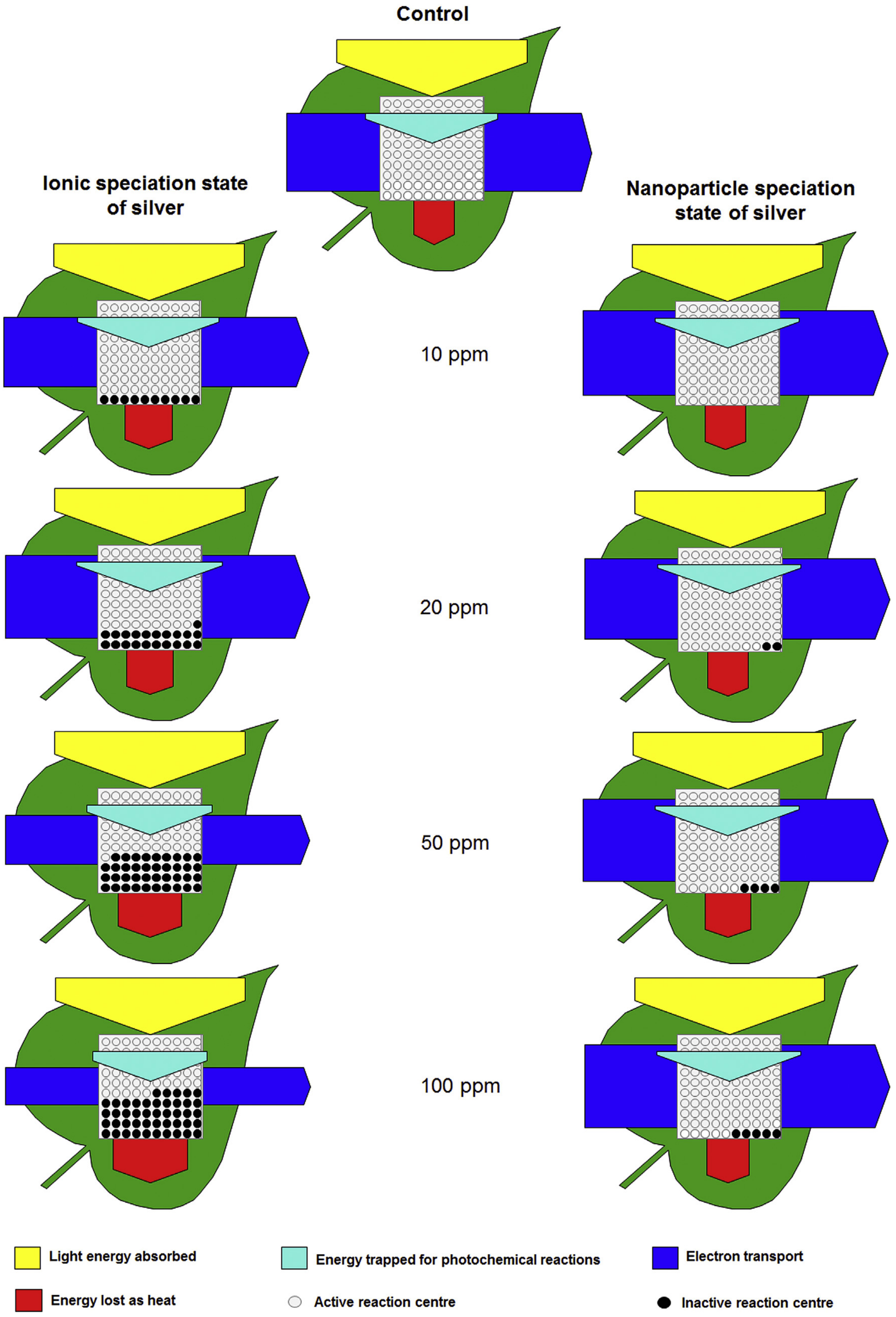

Fig. 5. Phenomenological yield models of wheat (*Triticum aestivum*) plants exposed to ionic (Ag^+) and nanoparticulate (Ag-NP) species of silver for 24 h, depicting proportion of absorbed light (i) trapped for photochemical reactions; (ii) utilized for electron transport; and (iii) dissipated as heat. These models also project the proportion of reaction centers that (i) are in active state (open circles) and (ii) turned into inactive (closed) state.

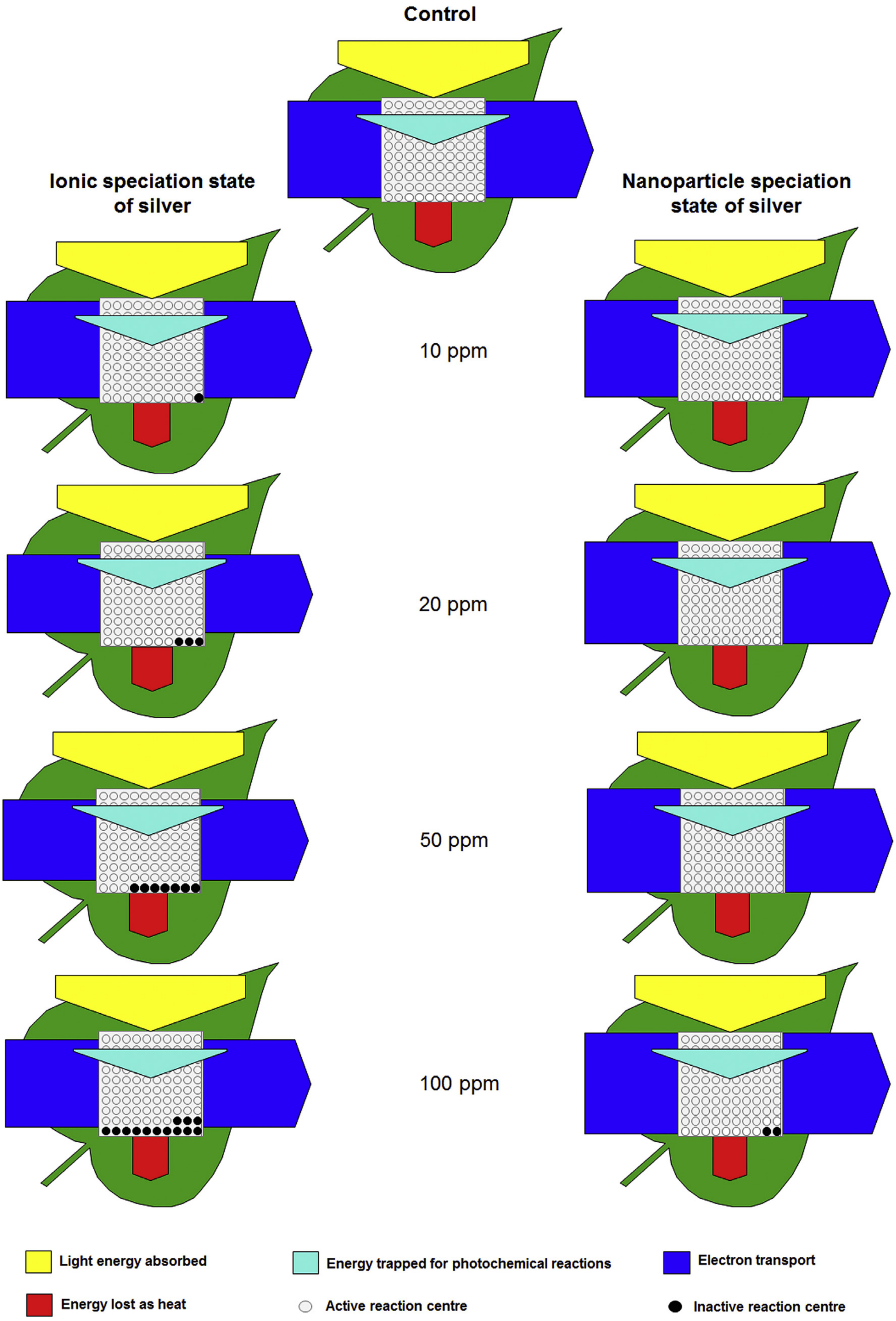

Fig. 6. Phenomenological yield models of sunflower (*Helianthus annuus*) plants exposed to ionic (Ag^+) and nanoparticle (Ag-NP) species of silver for 24 h, depicting proportion of absorbed light (i) trapped for photochemical reactions; (ii) utilized for electron transport; and (iii) dissipated as heat. These models also project the proportion of reaction centers that (i) are in active state (open circles) and (ii) turned into inactive (closed) state.

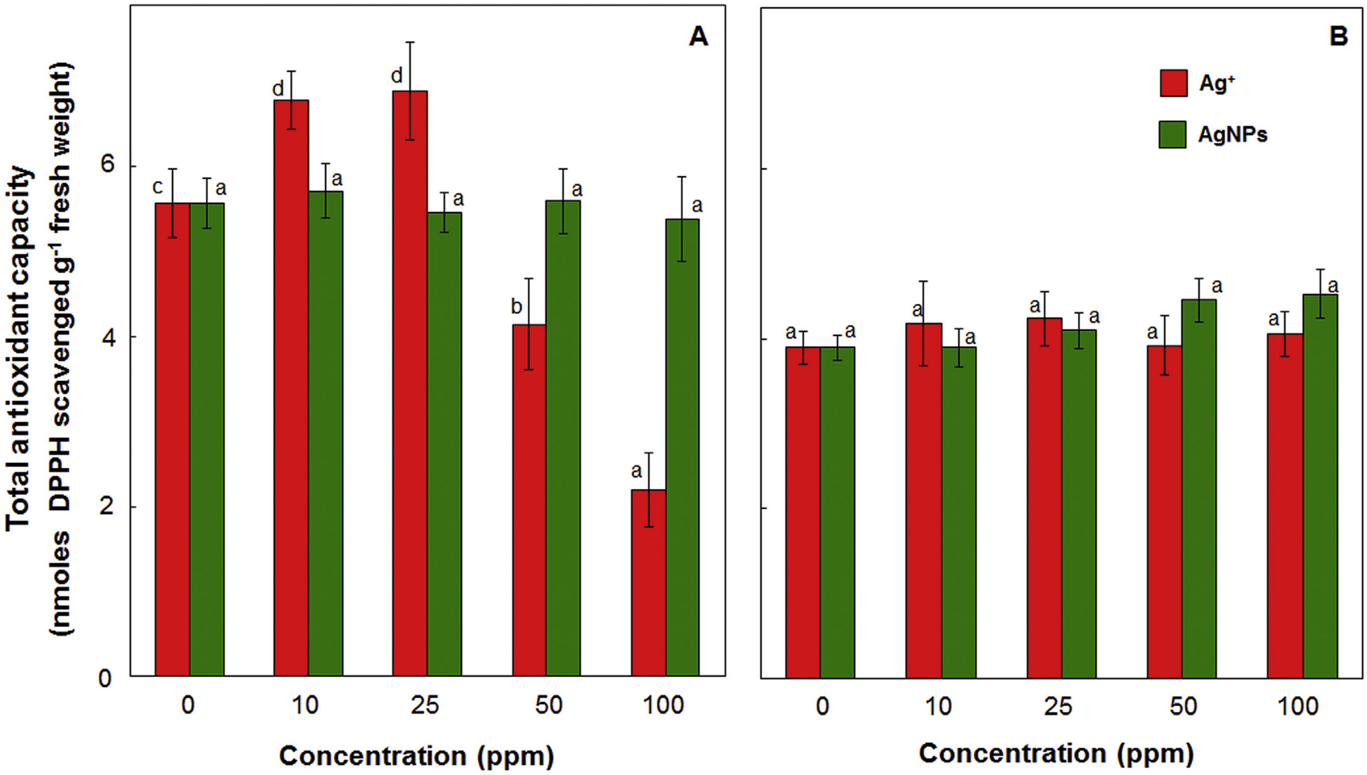

Fig. 7. Total antioxidant capacity (nmoles DPPH scavenged g^{-1} fresh weight) of leaves of wheat (A) and sunflower (B) plants exposed to varying concentrations of ionic (Ag^+) (red bars) and nanoparticulate (AgNPs) (green bars) species of silver for 24 h. Values represent mean of data collected from at least three independent experiments and vertical lines on bars represent standard error. Different small letters over the bars reflect that the values recorded for plants exposed to different concentrations (ppm) of Ag^+ or AgNPs differ significantly at $P < 0.05$ level (Duncan's multiple range test). (For interpretation of the references to colour in this figure legend, the reader is referred to the web version of this article.)

show a significant decline in antioxidants on exposure to Ag^+ (Shabnam et al., 2017b). The Ag^+-induced decline in the level of antioxidants has also been reported in other plant species (Xu et al., 2010). In the present study, we also observed a significant decline in the total antioxidant capacity in leaves of wheat plants exposed to Ag^+ at concentrations >50 ppm (Fig. 7). In contrast, leaves of sunflower plants exposed to Ag^+ did not show any significant variation in the total antioxidant capacity with respect to the control (Fig. 7). However, AgNPs did not induce any change in the total antioxidant capacity of leaves of either of the plants (Fig. 7). A number of researchers have reported potential of AgNPs generated through plant extracts to possess antioxidant capacity (Kokila et al., 2016; Venkatesan et al., 2016; Elemike et al., 2017).

3.4. *Silver content in plants*

Significant difference in the impacts of exogenously applied Ag^+ and AgNPs on PS II efficiency and related steps of Chl *a* fluorescence transients in wheat and sunflower leaves prompted us to determine silver content in these plants. Irrespective of the plants used and the concentration tested, Ag content was significantly higher in the plants exposed to Ag^+ than those exposed to AgNPs (Fig. 8). Similar findings were also reported in the studies with free floating *Spirodela polyrhiza* carried out by Jiang et al. (2012) and Shabnam et al. (2017). Higher levels of Ag in plants exposed to Ag^+ than in those exposed to AgNPs clearly revealed that absorption/uptake and translocation of Ag^+ were significantly higher than those of AgNPs. This could be a reason for the significantly higher negative impact of exogenously applied Ag^+ on plants than that of AgNPs. Among the two plants, i.e., wheat and sunflower, silver content was several times higher in the former than the latter, suggesting the potential of sunflower to restrict the uptake of Ag to be superior over that of wheat.

Interestingly, in the case of wheat, the Ag content was significantly higher in the root system compared to that in shoots (Fig. 8A and B). For instance, when exposed to 100 ppm Ag^+ or AgNPs, the level of Ag was about 8–12 times higher in roots that those in shoots. At the highest concentration of Ag^+ and AgNPs tested (i.e. 100 ppm), the Ag content in wheat leaves was ~0.8 and 0.3 mg g^{-1} dry weight, respectively. In the case of sunflower, however, Ag contents in roots and in shoots were similar. This clearly reveals that the root system of wheat has a superior filtration and retention capacity (i.e., rhizofiltration), compared to that of sunflower. In addition, it pinpoints towards the fact that the root system of wheat has a superior potential of accumulating/filtering Ag and, thus, restrict larger proportion of Ag to the root. Insignificant variation in photosynthetic efficiency of cotyledonary leaves of sunflower seedlings exposed to Ag^+ and AgNPs (Figs. 2 and 3), despite the translocation of silver into shoots, prompted us to evaluate the levels of Ag in stem and leaves. Interestingly, as evident from Fig. 8D and inset in Fig. 8D, Ag in shoots was restricted to stem. No detectable level of Ag was found in leaves. In fact, silver content was significantly higher in the sunflower stem compared to that in its roots (Fig. 8C and D). Restricted translocation of Ag into leaves could be the reason behind the minimal negative impacts of exogenously applied Ag^+ or AgNPs on the photosynthetic machinery and antioxidant capacity in sunflower.

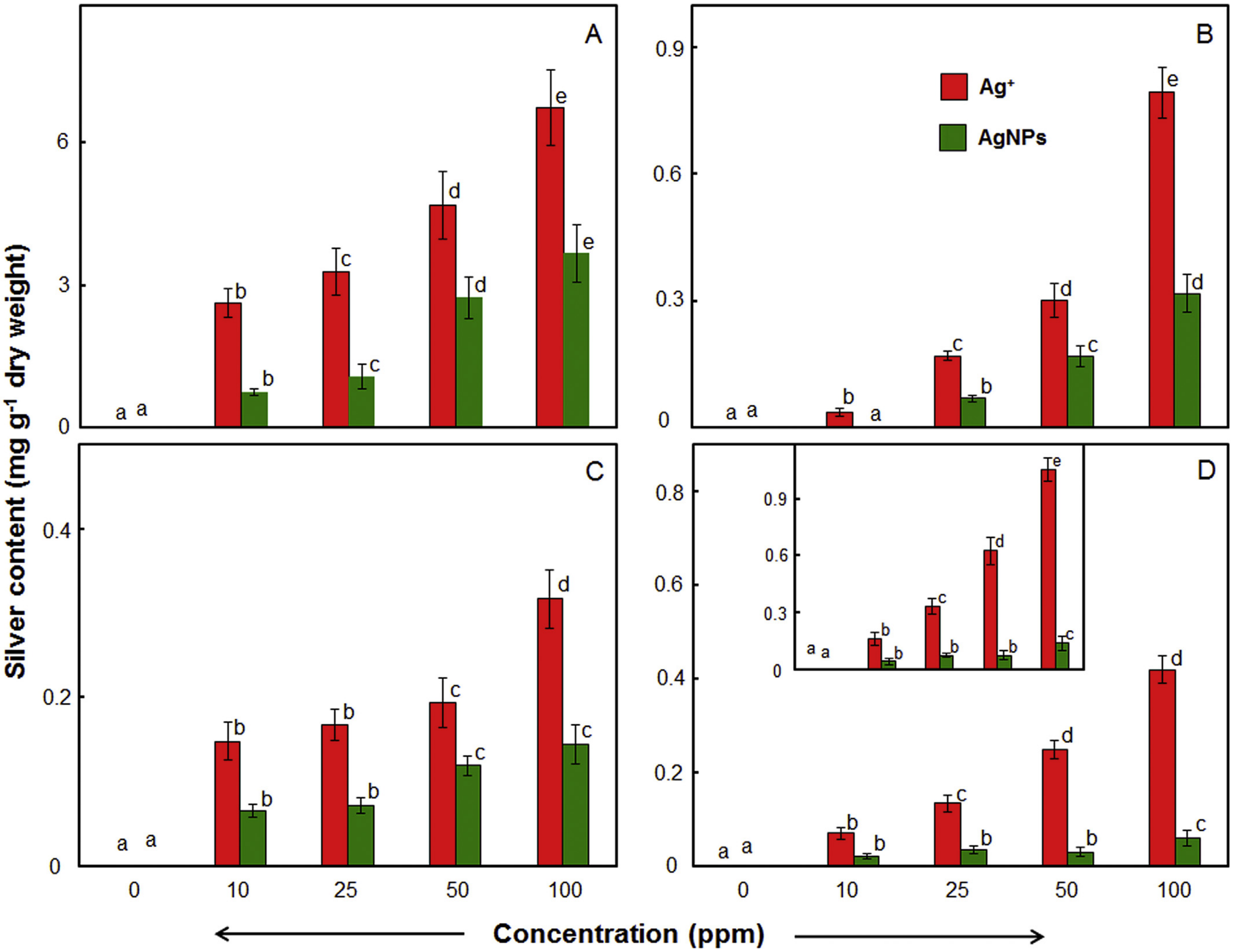

Fig. 8. Silver content in root (A, C) and shoot (B, D) of wheat (*Triticum aestivum*) (A, B) and sunflower (*Helianthus annuus*) (C, D) plants exposed to varying concentrations of ionic (Ag^+) (red bars) and nanoparticulate (AgNPs) (green bars) species of silver for 24 h. Inset in (D) represents silver content in stem of sunflower plants. Values represent mean of data collected from at least three independent experiments and vertical lines on bars represent standard error. Different small letters over the bars reflect that the values recorded for plants exposed to different concentrations (ppm) of Ag^+ or AgNPs differ significantly at $P < 0.05$ level (Duncan's multiple range test). (For interpretation of the references to colour in this figure legend, the reader is referred to the web version of this article.)

4. Conclusion

Present investigations revealed for the first time that (i) wheat is more sensitive to Ag^+ compared to sunflower, as Ag was translocated into leaves in the former but was detained by the stem in the latter. Accordingly, light harnessing photosynthetic events in the former were significantly suppressed, while those in the latter were least affected; (ii) absorption/translocation of Ag^+ was significantly higher than that of AgNPs in both plants, and accordingly, photosynthetic events even in wheat got least affected by AgNPs. In short, our findings clearly demonstrate that AgNPs are less/non-toxic to light harnessing photosynthetic events and total antioxidant potential of crop plants.

Acknowledgements

This work is supported by financial assistance from the Department of Biotechnology (Government of India) under Bio-CARe Women Scientist Scheme to P. Sharmila. H. Kim appreciates financial support from Korea Environmental Industry & Technology Institute (Project No: 2015001790002).

References

Ahamed, M., Alsalhi, M.S., Siddiqui, M.K., 2010. Silver nanoparticle applications and human health. Clin. Chim. Acta 411, 1841–1848.
Arruda, S.C.C., Silva, A.L.D., Galazzi, R.M., Azevedo, R.A., Arruda, M.A.Z., 2015. Nanoparticles applied to plant science: a review. Talanta 131, 693–705.
Bao, H., Yu, X., Xu, C., Li, X., Li, Z., Wei, D., Liu, Y., 2015. New toxicity mechanism of silver nanoparticles: promoting apoptosis and inhibiting proliferation. PLoS One 10, e0122535.
Benn, T.M., Westerhoff, P., 2008. Nanoparticle silver released into water from commercially available sock fabrics. Environ. Sci. Technol. 42, 4133–4139.
Brand-Williams, W., Cuvelier, M.E., Berset, C., 1995. Use of a free radical method to evaluate antioxidant activity. Lebensm. Wiss. Technol 18, 25–30.
Chae, Y.J., Chi Pham, C.H., Lee, J., Bae, E., Yi, J., Gu, M.B., 2009. Evaluation of the toxic impact of silver nanoparticles on Japanese medaka (*Oryzias latipes*). Aquat. Toxicol. 94, 320–327.
Chen, S., Yang, J., Zhang, M., Strasser, R.J., Qiang, S., 2016. Classification and characteristics of heat tolerance in *Ageratina Adenophora* populations using fast chlorophyll a fluorescence rise O-J-I-P. Environ. Exp. Bot. 122, 126–140.
Duvall, M., Wyatt, A., 2011. Regulation of Nanotechnology and Nanomaterials at EPA

and Around the World: Recent Developments and Context, Beveridge & Diamond, PC, Washington, DC, USA.

Elemike, E.E., Fayemi, O.E., Ekennia, A.C., Onwudiwe, D.C., Ebenso, E.E., 2017. Silver nanoparticles mediated by *Costus afer* leaf extract: synthesis, antibacterial, antioxidant and electrochemical properties. Molecules 22, 701.

Ellis, L.-J.A., Baalousha, M., Valsami-Jones, E., Lead, J.R., 2018. Seasonal variability of natural water chemistry affects the fate and behaviour of silver nanoparticles. Chemosphere 191, 616–625.

Fabrega, J., Luoma, S.N., Tyler, C.R., Galloway, T.S., Lead, J.R., 2011. Silver nanoparticles: behaviour and effects in the aquatic environment. Environ. Int. 3, 517–531.

Gondikas, A.P., von der Kammer, F., Reed, R.B., Wagner, S., Ranville, J.F., 2014. Release of TiO_2 nanoparticles from sunscreens into surface waters: a one-year survey at the old Danube recreational lake. Environ. Sci. Technol. 48, 5415–5422.

Gubbins, E.J., Batty, L.C., Lead, J.R., 2011. Phytotoxicity of silver nanoparticles to *Lemna minor* L. Environ. Poll. 159, 1551–1559.

Jiang, H.S., Li, M., Chang, F.-Y., Li, W., Yin, L.-Y., 2012. Physiological analysis of silver nanoparticles and $AgNO_3$ toxicity to *Spirodela polyrhiza*. Environ. Toxicol. Chem. 31, 1880–1886.

Kaegi, R., Sinnet, B., Zuleeg, S., Hagendorfer, H., Mueller, E., Vonbank, R., Boller, M., Burkhardt, M., 2010. Release of silver nanoparticles from outdoor facades. Environ. Poll. 158, 2900–2905.

Kalaji, H.M., Govindjee, Bosa, K., Koscielniak, J., Zuk-Golaszewskae, K., 2011. Effects of salt stress on photosystem II efficiency and CO_2 assimilation of two Syrian barley landraces. Environ. Exp. Bot. 73, 64–72.

Kokila, T., Ramesh, P.S., Geetha, D., 2016. Biosynthesis of AgNPs using Carica Papaya peel extract and evaluation of its antioxidant and antimicrobial activities. Ecotoxicol. Environ. Saf. 134, 467–473.

Kumari, M., Mukherjee, A., Chandrasekaran, N., 2009. Genotoxicity of silver nanoparticles in *Allium cepa*. Sci. Total Environ. 407, 5243–5246.

Kunniger, T., Gerecke, A.C., Ulrich, A., Huch, A., Vonbank, R., 2014. Release and environmental impact of silver nanoparticles and conventional organic biocides from coated wooden façades. Environ. Pol. 184, 464–471.

Lapresta-Fernández, A., Fernández, A., Blasco, J., 2012. Nanoecotoxicity effects of engineered silver and gold nanoparticles in aquatic organisms. Trends Anal. Chem. 32, 40–59.

Lin, D.H., Xing, B.S., 2007. Phytotoxicity of nanoparticles: inhibition of seed germination and root growth. Environ. Pol. 150, 243–250.

McDaniel, B.K., Binder, B.M., 2012. Ethylene receptor 1 (ETR1) is sufficient and has the predominant role in mediating inhibition of ethylene responses by silver in *Arabidopsis thaliana*. J. Biol. Chem. 287, 26094–26103.

Nair, P.M.G., Chung, I.M., 2014. Physiological and molecular level effects of silver nanoparticles exposure in rice (*Oryza sativa* L.) seedlings. Chemosphere 112, 105–113.

Navarro, E., Piccapietra, F., Wagner, B., Marconi, F., Kaegi, R., Odzak, N., Sigg, L., Behra, R., 2008. Toxicity of silver nanoparticles to *Chlamydomonas reinhardtii*. Environ. Sci. Technol. 42, 8959–8964.

Nel, A., Xia, T., Adler, N.M., Li, N., 2006. Toxic potential of materials at the nano-level. Science 311, 622–627.

Oukarroum, A., Barhoumi, L., Pirastru, L., Dewez, D., 2013. Silver nanoparticle toxicity effect on growth and cellular viability of the aquatic plant *Lemna gibba*. Environ. Toxicol. Chem. 32, 902–907.

Oukarroum, A., Polchtchikov, S., Perreault, F., Popovic, R., 2012. Temperature influence on silver nanoparticles inhibitory effect on photosystem II photochemistry in two green algae, *Chlorella vulgaris* and *Dunaliella tertiolecta*. Environ. Sci. Pollut. Res. 19, 1755–1762.

Pardha-Saradhi, P., Yamal, G., Peddisetty, T., Sharmila, P., Nagar, S., Singh, J., Nagarajan, R., Rao, K.S., 2014. Reducing strength prevailing at root surface of plants promotes reduction of Ag^+ and generation of Ag^0/Ag_2O nanoparticles exogenously in aqueous phase. PLoS One 9, e106715.

Qian, H., Peng, X., Han, X., Ren, J., Sun, L., Fu, Z., 2013. Comparison of the toxicity of silver nanoparticles and silver ions on the growth of terrestrial plant model *Arabidopsis thaliana*. J. Environ. Sci. 25, 1947–1955.

Rai, M., Yadav, A., Gade, A., 2009. Silver nanoparticles as a new generation of antimicrobials. Biotechnol. Adv. 27, 76–83.

Shabnam, N., Pardha-Saradhi, P., 2016. Floating and submerged leaves of *Potamogeton nodosus* exhibit distinct variation in antioxidant capacity as an ecophysiological adaptive strategy. Funct. Plant Biol. 43, 346–355.

Shabnam, N., Sharmila, P., Kim, H., Pardha-Saradhi, P., 2016. Light mediated generation of silver nanoparticles by spinach thylakoids/chloroplasts. PLoS One, e0167937.

Shabnam, N., Sharmila, P., Pardha-Saradhi, P., 2017. Impact of ionic and nanoparticle speciation states of silver on light harnessing photosynthetic events in *Spirodela polyrhiza*. Int. J. Phytoremed 19, 80–86.

Shabnam, N., Sharmila, P., Govindjee, Kim, H., Pardha-Saradhi, P., 2017b. Differential response of floating and submerged leaves of long leaf pondweed, Potamogeton nodosus, to silver ions. Front. Plant Sci. 8, 1052.

Shabnam, N., Sharmila, P., Sharma, A., Strasser, R.J., Govindjee, Pardha-Saradhi, P., 2015. Mitochondrial electron transport protects floating leaves of long leaf pondweed (*Potamogeton nodosus* Poir) against photoinhibition: comparison with submerged leaves. Photosynth. Res. 125, 305–319.

Sharma, P., Bhatt, D., Zaidi, M.G.H., Pardha-Saradhi, P., Khanna, P.K., Arora, S., 2012. Silver nanoparticle mediated enhancement in growth and antioxidant status of *Brassica juncea*. Appl. Biochem. Biotech. 167, 2225–2233.

Stampoulis, D., Sinha, S.K., White, J.C., 2009. Assay-dependent phytotoxicity of nanoparticles to plants. Environ. Sci. Technol. 43, 9473–9479.

Strasser, B.J., Strasser, R.J., 1995. Measuring fast fluorescence transients to address environmental questions: the JIP-test. In: Mathis, P. (Ed.), Photosynthesis: from Light to Biosphere. Kluwer Academic Publishers, The Netherlands, pp. 977–980.

Strasser, R.J., Srivastava, A., Tsimilli-Michael, M., 2004. Analysis of the chlorophyll a fluorescence transient. In: Papageorgiou, G., Govindjee (Eds.), Advances in Photosynthesis and Respiration. Springer, The Netherlands, pp. 321–362.

Thuesombat, P., Hannongbua, S., Akasit, S., Chadchawan, S., 2014. Effect of silver nanoparticles on rice (*Oryza sativa* L. cv. KDML105) seed germination and seedling growth. Ecotoxicol. Environ. Saf. 104, 302–309.

Vani, B., Pardha-Saradhi, P., Mohanty, P., 2001. Characterization of high temperature induced stress impairments in thylakoids of rice seedlings. Indian J. biochem. Biophys. 38, 220–229.

Vannini, C., Domingo, G., Onelli, E., Mattia, F.D., Bruni, I., Marsoni, M., Bracale, M., 2014. Phytotoxic and genotoxic effects of silver nanoparticles exposure on germinating wheat seedlings. J. Plant Physiol. 171, 1142–1148.

Venkatesan, J., Kim, S.K., Shim, M.S., 2016. Antimicrobial, antioxidant, and anticancer activities of biosynthesized silver nanoparticles using marine algae *Ecklonia cava*. Nanomaterials 6, 235.

Xu, Q.S., Hu, J.Z., Xie, K.B., Yang, H.Y., Du, K.H., Shi, G.X., 2010. Accumulation and acute toxicity of silver in Potamogeton crispus L. J. Hazard. Mater. 173, 186–193.

Yamal, G., Sharmila, P., Rao, K.S., Pardha-Saradhi, P., 2013. Inbuilt potential of YEM medium and its constituents to generate Ag/Ag_2O nanoparticles. PLoS One 8, e61750.

Yasur, J., Rani, P.U., 2013. Environmental effects of nano-silver: impact on castor seed germination, seedling growth, and plant physiology. Environ. Sci. Pollut. Res. 20, 8636–8648.

Yin, L., Colman, B.P., McGill, B.M., Wright, J.P., Bernhardt, E.S., 2012. Effects of silver nanoparticle exposure on germination and early growth of eleven wetland plants. PLoS One 7, e47674.

Yin, L., Cheng, Y., Espinasse, B., Colman, B.P., Auffan, M., Wiesner, W., Rose, J., Liu, J., Bernhardt, E.S., 2011. More than the ions: the effects of silver nanoparticles on *Lolium multiflorum*. Environ. Sci. Technol. 45, 2360–2367.

Zhang, M., Shan, Y.J., Kochian, L., Strasser, R.J., Chen, G., 2015. Photochemical properties in flag leaves of a super-high-yielding hybrid rice and a traditional hybrid rice (*Oryza sativa* L.) probed by chlorophyll a fluorescence transient. Photosynth. Res. 126, 275–284.

Zhao, C.M., Wang, W.X., 2011. Comparison of acute and chronic toxicity of silver nanoparticles and silver nitrate to *Daphnia magna*. Environ. Toxicol. Chem. 30, 885–892.

Zuverza-Mena, N., Armendariz, R., Peralta-Videa, J.R., Gardea-Torresdey, J.L., 2016. Effects of silver nanoparticles on radish sprouts: root growth reduction and modifications in the nutritional value. Front. Plant Sci. 7, 90.